MECSOL 2022 - Proceedings of the 8th International Symposium on Solid Mechanics
M.L. Bittencourt, J. Labaki, L.C.M. Vieira Jr. and E. Mesquita (Editors), Campinas SP, Brazil, October 17th to 19th, 2022

Modeling and Analysis of Active/Passive Vehicle Vibration Attenuation System under Different Road Excitations

Leonardo Roso Colpo [1] and Herbert Martins Gomes [1]

[1] Federal University of Rio Grande do Sul, Department of Mechanical Engineering, Sarmento Leite St., 425 - Room 202, 90040-001, Porto Alegre, RS, Brazil.

Abstract: The key function of a suspension system in a vehicle is to isolate the passengers from the vibrations originating from the ground, besides guaranteeing the vehicle stability by maintaining all tires in contact. This is usually a trade-off since comfort and stability are conflicting goals which require opposite directions on suspension parameters tuning. Standard suspension designs have only spring and shock absorber elements that can be determined to be efficient in a small range of conditions since they can't adapt and control forces due to necessity. To overcome these barriers, intelligent suspension designs are developed, changing its parameters or adding energy to increase the vehicle's performance. The best acceleration reduction and road holding results are achieved using active suspensions, which exert forces in the system using actuators. In the most common applications, an actuator is placed on each suspension attached to the wheels. The disadvantages of these systems are the high cost of their elements and the large amount of energy required to achieve the performance goals. A potentially viable solution to overcome cost and energy issues in active suspensions is to change the approach of the suspension concept, placing the actuators on the seat of the occupants. This strategy may provide equal performance with considerably less energy, making the active system more viable. This paper proposes a performance study on vibration attenuation of a full car suspension system. The traditional passive system is used initially under road roughness (ISO 8608:1995) and bumps. Then a classic active system is developed, based on Literature references, using a Linear Quadratic Regulator (LQR) to attenuate vibration using actuators on each wheel. Moreover, an active seat model is developed and tuned to achieve the best performance and latter compared to the other systems. Time histories for chassis and driver's seat accelerations are presented, and the systems' control forces and relative performance are compared. Acceleration transmissibility shows the effectiveness and advantages of using such approach.

Keywords: Active suspension, Vibration attenuation, Vehicle suspension, Random Excitations

INTRODUCTION

The attenuation of vibration levels on vehicle occupants is one of the main fields of research in the automotive industry since its perception is directly related to customer satisfaction and purchasing decisions (Karen et al., 2012; Patelli et al., 2018). Moreover, the exposition of specific vibration levels can be harmful to the health of the occupants depending on time exposure. Those effects are studied in the early design stages of vehicle development by dynamic models of the suspension system, which can predict the chassis's response due to external excitations and allow to determine the best parameters for higher ride quality (Mahala et al., 2009). Many models are used to represent vibrational effects on a vehicle, which can change from a simple linear model to multiple degrees of freedom (DOF) with non-linearities to understand and evaluate non-trivial effects in the vehicle's ride.

The most common way to design a suspension system is with a passive system, with no strategy or control acting in the system. Passive suspensions rely only on fixed parameters such as damping and stiffness, which cannot be changed due to vehicle handling constraints. That means that passive systems can be tuned to optimize vibration attenuation at a small range of conditions, giving a poor performance on general utilization with variations of excitations, payloads, and vehicle speed. To achieve better results on passive systems, vehicle developers often use strategies to benefit from the nonlinear behavior of suspension parameters, especially damping effects. Recent work (Colpo and de Souza, 2020) showed that manipulating oil flow inside shock absorbers could reduce 33% of accelerations transmitted to the vehicle occupants. These manipulations can be made by position-sensitive oil passages (Łuczko and Ferdek, 2020), a connection between oil chambers (Ferdek and Łuczko, 2018), and asymmetrical dampers (Jia et al., 2019). All strategies considerably attenuate vibrational levels, but only by enlarging the suspension system's effective range of conditions may present substantial attenuation. To efficiently attenuate vibrations levels transmitted to the vehicle occupants, there is a need to develop intelligent suspension systems.

Unlike passive systems, intelligent suspension systems can self-adapt to external conditions without driver interference. There are two categories of intelligent systems: active and semi-active suspensions. As long as semi-active

systems can change vehicle properties in real-time, active systems can add energy to stabilize vibrations (Liu et al., 2013). For example, a semi-active system can change the density of a magneto-rheological fluid (Li et al., 2021) as long as an active suspension can exert forces in the system by a pneumatic actuator (Ho and Ahn, 2021). Even though active suspensions are more complex and costly, they are the foremost field in research due to the results that can be achieved with their application (Xue et al., 2011). Semi-active and active systems, both categories need the understanding of how to best act due to the random excitations being applied to the vehicle. The system works by following a control law that defines how the system will react to external excitations and how much energy can be put into the system (in the case of active suspensions).

A widespread control strategy is the Linear Quadratic Regulator (LQR), which many researchers have used to control an active suspension system. Sam et al. (2000) investigated the benefits of an LQR controller in an active suspension, attesting it as a solution of comfort and handling quality for vehicles. More recent studies (Chen and Chen, 2021; S. and K., 2019) showed that LQR is still a viable solution to attenuate vehicle vibrations, achieving excellent solutions for the ride, handling, and suspension settling time. LQR controllers can even perform better than current intelligent strategies such as Fuzzy Logic (FL), as shown in (Hasbullah and Faris, 2010), with the downside of consuming more energy to attenuate vehicle vibration.

The amount of consumed energy is one of the main concerns for the active suspensions and the design of the actuators. It is common to evaluate the total energy required for the active suspension with a full car dynamic model that comprehends all wheels and chassis properties on the simulations. The utilization of a full car model for active suspensions was performed in several works (Chen and Chen, 2021; Haemers et al., 2018; Shirahatt et al., 2008) because it can predict the force of each actuator, usually attached to the suspension of each wheel. This approach can achieve good results in vibration attenuation and handling quality due to the individual control of each wheel. Nevertheless, the high number of actuators and sensors required is not affordable, besides the high energy consumption.

Alternatives for cheaper and less energy-consuming systems are being discussed to address these issues. Instead, one of these alternatives is not placing actuators and controllers in the suspension but putting them on the occupant's seat. Heidarian and Wang (2019) researched technologies for seat vibration control, where the active seat was shown as the best choice. An active seat needs fewer controllers and sensors, besides being likely to consume less energy due to forces magnitude, especially in heavy vehicles. Yu et al. (2008) discussed an active seat for an agricultural tractor, and Kineke et al. (2013) designed an active seat for military vehicles. Both works achieved a significant reduction in vibration levels when compared to passive systems. Al-Ashmori and Wang (2020) performed a systematic literature survey of active seat methods for heavy trucks, attesting the strategy as a trend for vehicle vibration attenuation.

This work comprehends the analysis of an active seat system and its results when compared to the passive suspension system, as well as a comparison in terms of spent energy and vibration attenuation with a usual active suspension. The vehicle is modeled by the full car model with the driver seat, and road bumps and random vibrations due to road roughness uses ISO 8608:1995 recommendations. The total vibration level at the driver seat is evaluated (ISO 2631-1:1997) and compared to the proposed solutions and literature results. Finally, the comparisons with the total energy expenditures are made, and final discussions are traced.

Vehicle models

An 8 DOF full car model with a driver seat will be considered in the analysis of this work, similar to the model found in (Shirahatt et al., 2008). All vehicle properties are the same as that found in this article.

Active and Passive Suspension

The active model will be described in this section. The passive system description is the same, only considering the actuator's forces as zero or the gain matrix to be null. More details are in the controller design section. Figure 1 shows the representation of the model, where m_p is the seat mass; m is the chassis sprung mass; I_x and I_y the inertial moments in each axle; w is the vehicle gauge; a is the distance of the front axle to the center of gravity (CG); b is the distance from the rear axle to the CG; x_p is the longitudinal distance between the seat and the CG; y_p is the transversal distance between the seat and CG; z_p is the seat vertical displacement; z is the chassis vertical displacement; φ is the chassis roll angle; θ is the chassis pitch angle; z_i is the vertical displacement of each wheel, where the index 1 is for the front left wheel; 2 is for the rear left wheel; 3 is for the front right wheel, and 4 is for the rear right wheel. Also, k_i is the suspension stiffness in each wheel; c_i is the damping of each suspension; k_{ti} is the stiffness from each tire; u_{bi} is the ground displacement in each wheel, and f_{ai} is the actuator force in each suspension. Finally, c_p is the seat damping, and k_p is the seat stiffness.

The equation of motion for the vehicle seat is given by:

$$m_p \ddot{z}_p = k_p \left(z - z_p + \phi y_p - \theta x_p \right) + c_p \left(\dot{z} - \dot{z}_p + \dot{\phi} y_p - \dot{\theta} x_p \right) \tag{1}$$

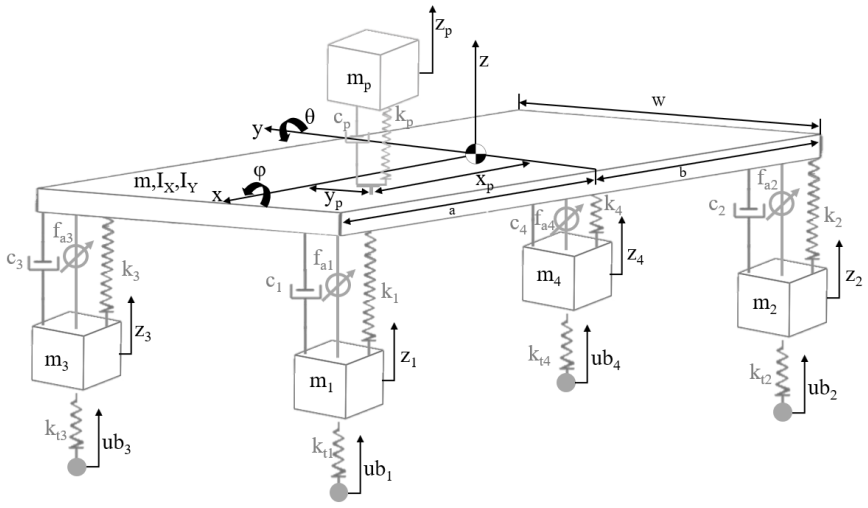

Figure 1 - Full car active suspension model

For the chassis vertical displacement:

$$\begin{aligned} &m\ddot{z} = k_p\left(-z+z_p-\phi y_p+\theta x_p\right)+c_p\left(-\dot{z}+\dot{z}_p-\dot{\phi}y_p+\dot{\theta}x_p\right)+k_1\left(-z+z_1-\phi\frac{w}{2}+\theta a\right)+\ldots \\ &c_1\left(-\dot{z}+\dot{z}_1-\dot{\phi}\frac{w}{2}+\dot{\theta}a\right)+k_2\left(-z+z_2-\phi\frac{w}{2}-\theta b\right)+c_2\left(-\dot{z}+\dot{z}_2-\dot{\phi}\frac{w}{2}-\dot{\theta}b\right)+\ldots \\ &k_3\left(-z+z_3+\phi\frac{w}{2}+\theta a\right)+c_3\left(-\dot{z}+\dot{z}_3+\dot{\phi}\frac{w}{2}+\dot{\theta}a\right)+k_4\left(-z+z_4+\phi\frac{w}{2}-\theta b\right)+\ldots \\ &c_4\left(-\dot{z}+\dot{z}_4+\dot{\phi}\frac{w}{2}-\dot{\theta}b\right)+f_{a_1}+f_{a_2}+f_{a_3}+f_{a_4} \end{aligned} \tag{2}$$

For chassis roll:

$$\begin{aligned} &I_X\ddot{\phi} = k_p y_p\left(-z+z_p-\phi y_p+\theta x_p\right)+c_p y_p\left(-\dot{z}+\dot{z}_p-\dot{\phi}y_p+\dot{\theta}x_p\right)+k_1\frac{w}{2}\left(-z+z_1-\phi\frac{w}{2}+\theta a\right)+\ldots \\ &c_1\frac{w}{2}\left(-\dot{z}+\dot{z}_1-\dot{\phi}\frac{w}{2}+\dot{\theta}a\right)+k_2\frac{w}{2}\left(-z+z_2-\phi\frac{w}{2}-\theta b\right)+c_2\frac{w}{2}\left(-\dot{z}+\dot{z}_2-\dot{\phi}\frac{w}{2}-\dot{\theta}b\right)+\ldots \\ &k_3\frac{w}{2}\left(z-z_3-\phi\frac{w}{2}-\theta a\right)+c_3\left(\dot{z}-\dot{z}_3-\dot{\phi}\frac{w}{2}-\dot{\theta}a\right)+k_4\frac{w}{2}\left(z-z_4+\phi\frac{w}{2}+\theta b\right)+\ldots \\ &c_4\frac{w}{2}\left(\dot{z}-\dot{z}_4+\dot{\phi}\frac{w}{2}+\dot{\theta}b\right)+f_{a_1}\frac{w}{2}+f_{a_2}\frac{w}{2}-f_{a_3}\frac{w}{2}-f_{a_4}\frac{w}{2} \end{aligned} \tag{3}$$

For chassis pitch:

$$\begin{aligned} &I_Y\ddot{\theta} = k_p y_p\left(z-z_p+\phi y_p-\theta x_p\right)+c_p y_p\left(\dot{z}-\dot{z}_p+\dot{\phi}y_p-\dot{\theta}x_p\right)+k_1 a\left(z-z_1+\phi\frac{w}{2}-\theta a\right)+\ldots \\ &c_1 a\left(\dot{z}-\dot{z}_1+\dot{\phi}\frac{w}{2}-\dot{\theta}a\right)+k_2 b\left(-z+z_2-\phi\frac{w}{2}-\theta b\right)+c_2 b\left(-\dot{z}+\dot{z}_2-\dot{\phi}\frac{w}{2}-\dot{\theta}b\right)+\ldots \\ &k_3 a\left(z-z_3-\phi\frac{w}{2}-\theta a\right)+c_3 a\left(\dot{z}-\dot{z}_3-\dot{\phi}\frac{w}{2}-\dot{\theta}a\right)+k_4 b\left(-z+z_4+\phi\frac{w}{2}-\theta b\right)+\ldots \\ &c_4 b\left(-\dot{z}+\dot{z}_4+\dot{\phi}\frac{w}{2}-\dot{\theta}b\right)-f_{a_1}a+f_{a_2}b-f_{a_3}a+f_{a_4}b \end{aligned} \tag{4}$$

And for each unsprung mass:

$$m_1\ddot{z}_1 = k_1\left(z - z_1 + \phi\frac{w}{2} - \theta a\right) + c_1\left(\dot{z} - \dot{z}_1 + \dot{\phi}\frac{w}{2} - \dot{\theta}a\right) + k_{t_1}\left(u_{b_1} - z_1\right) - f_{a_1} \tag{5}$$

$$m_2\ddot{z}_2 = k_2\left(z - z_2 + \phi\frac{w}{2} + \theta b\right) + c_2\left(\dot{z} - \dot{z}_2 + \dot{\phi}\frac{w}{2} + \dot{\theta}b\right) + k_{t_2}\left(u_{b_2} - z_2\right) - f_{a_2} \tag{6}$$

$$m_3\ddot{z}_3 = k_3\left(z - z_3 - \phi\frac{w}{2} - \theta a\right) + c_3\left(\dot{z} - \dot{z}_3 - \dot{\phi}\frac{w}{2} - \dot{\theta}a\right) + k_{t_3}\left(u_{b_3} - z_3\right) - f_{a_3} \tag{7}$$

$$m_4\ddot{z}_4 = k_4\left(z - z_4 - \phi\frac{w}{2} + \theta b\right) + c_4\left(\dot{z} - \dot{z}_4 - \dot{\phi}\frac{w}{2} + \dot{\theta}b\right) + k_{t_4}\left(u_{b_4} - z_4\right) - f_{a_4} \tag{8}$$

Finally, in matrix form:

$$\mathbf{M}\ddot{z} + \mathbf{C}\dot{z} + \mathbf{K}z = \mathbf{F}u + \mathbf{K_e}u_b \tag{9}$$

For brevity purposes, the resulting coefficients of matrices **M**, **C,** and **K** will not be shown. The **Ke** matrix is defined by

$$\mathbf{K_e} = \begin{bmatrix} 0_{4x4} \\ diag\left\{k_{t_1}, k_{t_2}, k_{t_3}, k_{t_4}\right\} \end{bmatrix} \tag{10}$$

That multiplies the ground displacement vector u_b:

$$u_b = \begin{bmatrix} u_{b_1} & u_{b_2} & u_{b_3} & u_{b_4} \end{bmatrix}^T \tag{11}$$

The matrix **F** is defined by:

$$\mathbf{F} = \begin{bmatrix} 0 & 0 & 0 & 0 \\ 1 & 1 & 1 & 1 \\ \frac{w}{2} & \frac{w}{2} & -\frac{w}{2} & -\frac{w}{2} \\ -a & b & -a & b \\ -1 & 0 & 0 & 0 \\ 0 & -1 & 0 & 0 \\ 0 & 0 & -1 & 0 \\ 0 & 0 & 0 & -1 \end{bmatrix} \tag{12}$$

That multiplies the control forces vector *u*:

$$u = \begin{bmatrix} f_{a_1} & f_{a_2} & f_{a_3} & f_{a_4} \end{bmatrix}^T \tag{13}$$

Active Seat

The model with the active seat can is shown in Fig.2. The actuator is placed beneath the seat, exerting a force f_p in the model. For the active seat, matrices **M**, **C**, **K,** and $\mathbf{K_e}$ remain the same on the active suspension model and the ground excitation vector u_b. The difference is in the matrix **F**:

$$\mathbf{F} = \begin{bmatrix} -1 & 1 & y_p & -x_p & 0 & 0 & 0 & 0 \end{bmatrix}^T \tag{14}$$

And in the control force vector, which only contains the seat actuator force:

$$u = [\, f_p \,] \tag{15}$$

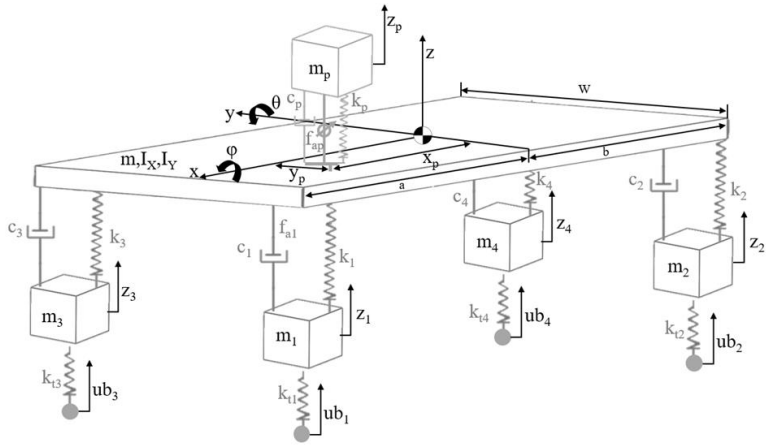

Figure 2 - Full car with active seat

To solve the system of differential equations, the equation of motion is written in the space-state form as:

$$\begin{cases} \dot{x} = \mathbf{A}x + \mathbf{B}u + \mathbf{G}u_b \\ y = \mathbf{C}_s x + \mathbf{D}u \end{cases} \tag{16}$$

where **A**, **B**, $\mathbf{C_s}$, and **D** are state-space matrices due to the state vector x, and y is the observation vector. The state vector x is defined by:

$$x = \begin{Bmatrix} z & \dot{z} \end{Bmatrix}^T \tag{17}$$

What gives the first line of Eq.(16) to be:

$$\dot{x} = \begin{bmatrix} \mathbf{0} & \mathbf{I} \\ -\mathbf{M}^{-1}\mathbf{K} & -\mathbf{M}^{-1}\mathbf{C} \end{bmatrix} \begin{Bmatrix} z \\ \dot{z} \end{Bmatrix} + \begin{bmatrix} 0 \\ \mathbf{M}^{-1}\mathbf{F} \end{bmatrix} \{u\} + \begin{bmatrix} 0 \\ \mathbf{M}^{-1}\mathbf{K_e} \end{bmatrix} \{u_b\} \tag{18}$$

The matrix $\mathbf{C_s}$ is an identity matrix, and the matrix **D** is null.

Ground Excitations

The road bumps analysis is made by two consecutive bumps apart λ = 20 m from each one, with height h = 0.05 m. The vehicle will perform the simulations at a speed of V = 20 m/s. The road profile, in that case, is given by:

$$u_{b1,3}(t) = \begin{cases} \frac{h}{2}\left(1-\cos\left(\omega t\right)\right), & \text{if } 0 \le t \le \frac{2\lambda}{V} \\ 0 & \text{Otherwise} \end{cases} \tag{19}$$

$$u_{b2,4}(t) = \begin{cases} \frac{h}{2}\left(1-\cos\left(\omega\left(t-\tau\right)\right)\right), & \text{if } \tau \le t \le \left(\tau + \frac{2\lambda}{V}\right) \\ 0 & \text{Otherwise} \end{cases} \tag{20}$$

Where τ is the delay between the front and rear axle hitting the obstacle, and ω is the profile roughness frequency in the time domain that is exerted by the bumps. Both can be described as:

$$\tau = \frac{a+b}{V} \qquad \omega = \frac{2\pi V}{\lambda} \tag{21}$$

In addition, the bumps are lagged in space to excite roll movements, hitting each wheel at a delay of 0.2 seconds. The resulting bumps are in Fig.3. That means u_{b3} and u_{b4} from Eq. (19) and Eq. (20) are delayed another 0.2 seconds in the bump generation. For the road profile, a random road of class C was generated accordingly to ISO 86308:1995, as seen in Fig.4. For checking purposes, Fig.5 shows the Power Spectral Density (PSD) of the generated irregularities against the class C definition in ISO 86308:1995.

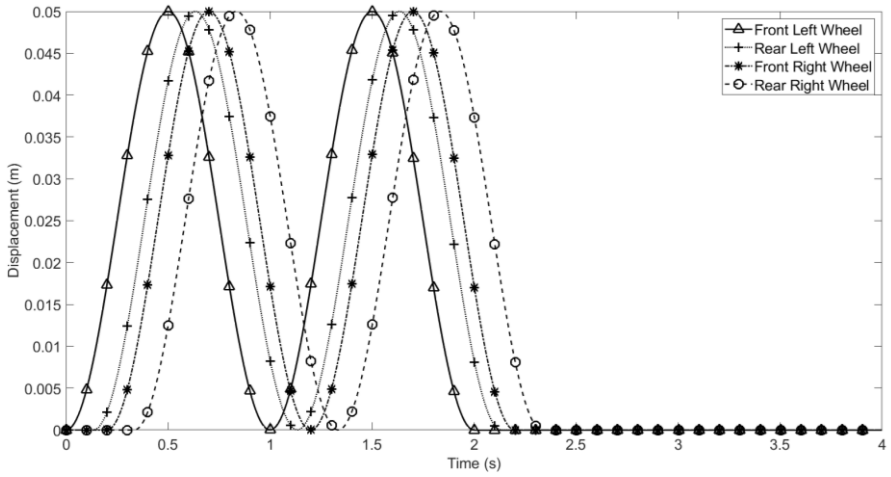

Figure 3 - Road bumps profiles [Adapted from Shirahatt(2008)]

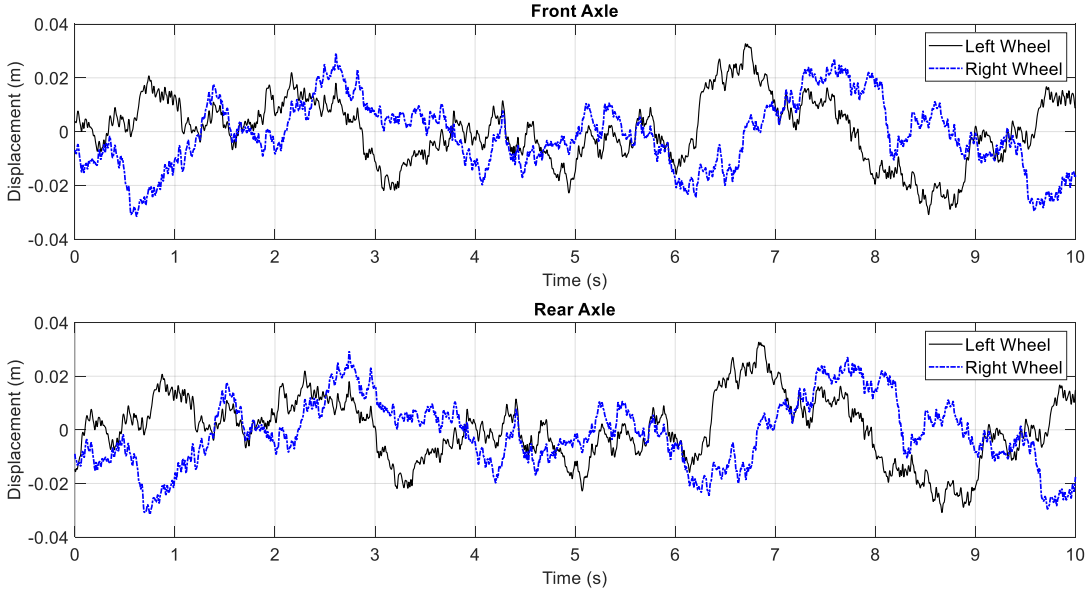

Figure 4 - Random vibration for front and rear wheels

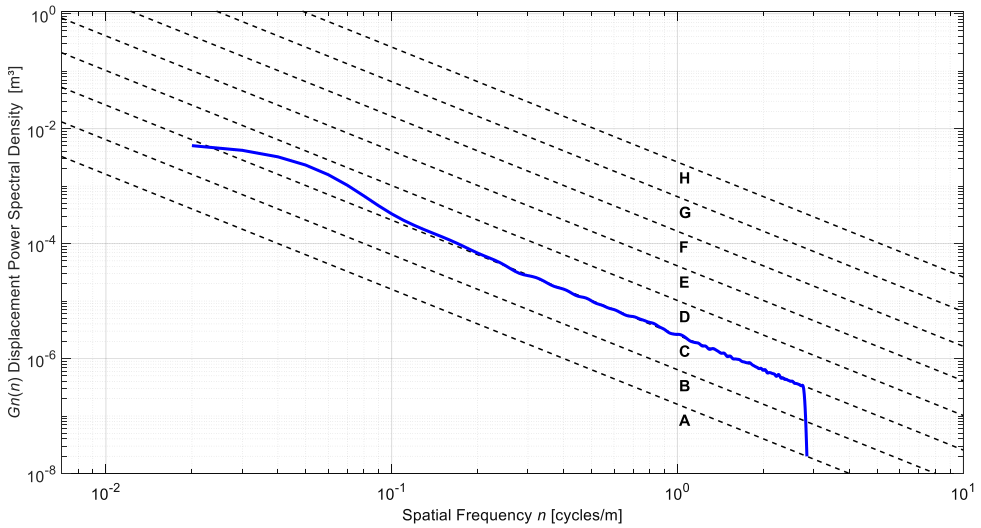

Figure 5 - Road class determination

Controller Design

The LQR controller is a strategy with gain values to the system translated into forces to minimize the system's total energy. This minimization is measured by a performance index J, given by:

$$J = \int_0^\infty \left(x'\mathbf{Q}x + u'\mathbf{R}u \right) dt \tag{22}$$

where **Q** and **R** are determined by the controller designer, the resulting control forces are given by:

$$u = -\mathbf{G}x \tag{23}$$

where u are the control forces and **G** is the gain matrix obtained by:

$$\mathbf{G} = \mathbf{R}^{-1}\mathbf{B}^T\mathbf{P} \tag{24}$$

where **P** is the matrix that satisfices the Riccati algebraic equation:

$$\mathbf{PA} + \mathbf{A}^T\mathbf{P} + \mathbf{Q} - \mathbf{PBR}^{-1}\mathbf{B}^T\mathbf{P} = 0 \tag{25}$$

The **G** matrix needs to be defined as null to perform a simulation with a passive suspension.

Vibration evaluation

The total level of vibration is evaluated with ISO 2631-1:1997 methodology, as follows:

$$a_v = \left(\sum_i^T \left(w_k a_w \right)^2 \right)^{\frac{1}{2}} \tag{26}$$

where a_v is the total weighted acceleration, a_w is the instantaneous weighted acceleration, T is the simulation time, and w_k is the weighting factors for the accelerations due to the frequency that is a function of the vibration direction (vertical at the seat).

Results and Discussion

For the bumps, the seat displacement results are in Fig.6 (a), and the acceleration results are in Fig.6 (b).

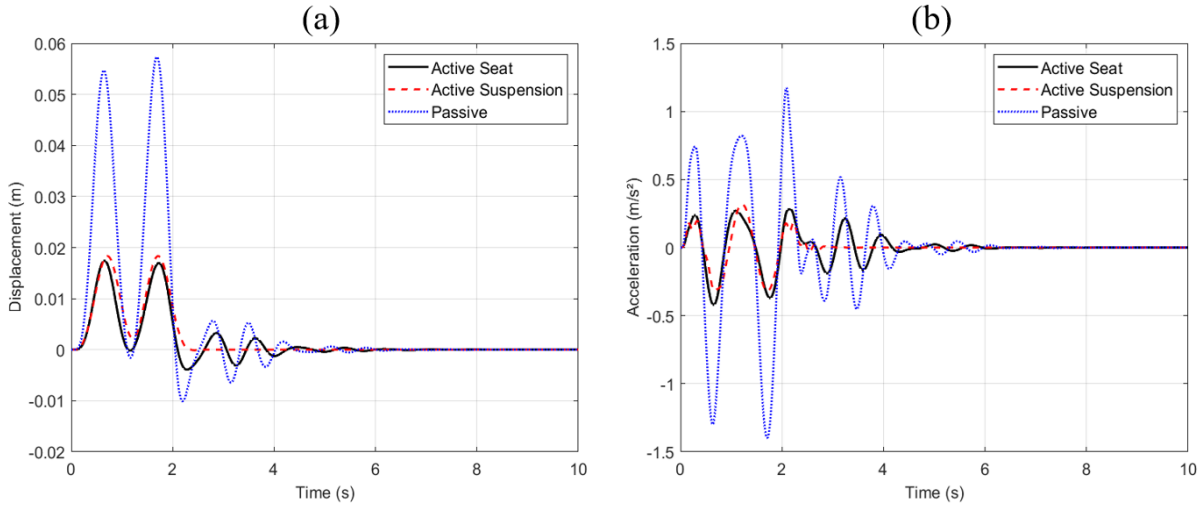

Figure 6 - Seat displacements over the bumps

It can be seen that the peak of displacements is very similar to both control strategies, with a reduction of 70% compared to the passive system. The active seat has a longer settling time since the active suspension can use four actuators to stabilize the system. The ISO class C road results are in Fig.7 for seat displacements and in Fig.8 for seat acceleration.

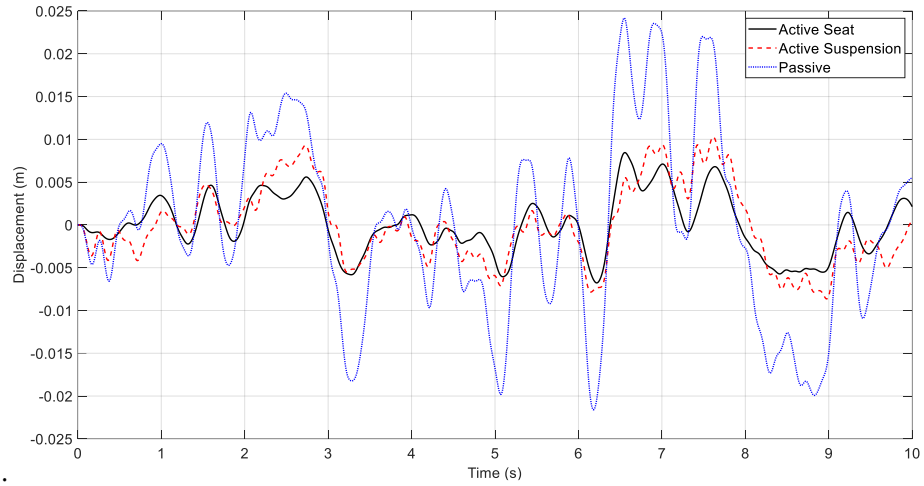

Figure 7 - Seat displacements over class C road

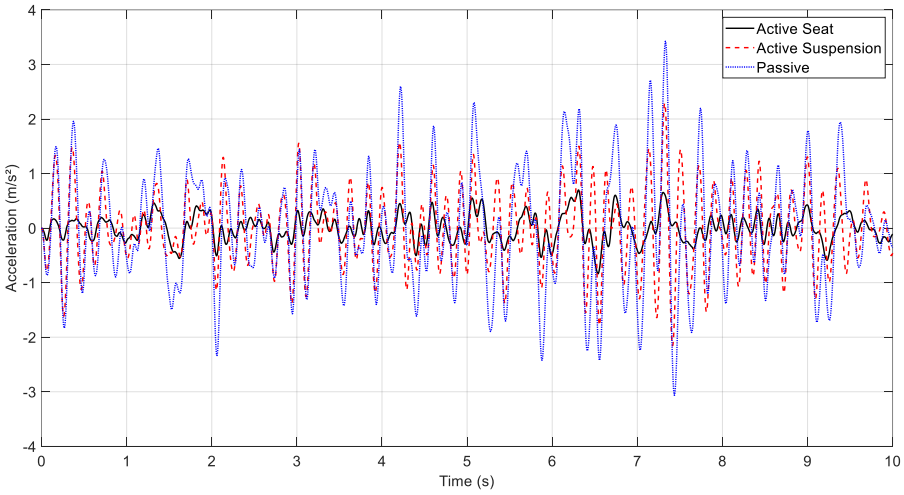

Figure 8 - Seat accelerations over class C road

It is possible to notice a considerable reduction in seat displacements with active systems. The active seat provides a smoother displacement than the active suspension, translated to a visible lower acceleration on the seat. The final values of acceleration for this case are in Tab.1. In the bumps, acceleration results show that the active system can attenuate a large part of the vibration transmitted to the driver, with 70% reduction for the active seat and 76% for the active suspension. This difference is due to the more significant settling time of the active seat. However, the seat consumes 0.003020 kWh of energy during the whole maneuver, as long as the suspension system consumes 0.007946 kWh. In the class C road, the active seat provides a reduction of 80% of the total value of acceleration, while the active suspension only reduces 20%. The total energy consumed for the time considered is 0.0115 kWh for the active seat and 0.1870 kWh for the active suspension.

Table 1 - Total acceleration values over the class C road

Case	Total acceleration a_v (m/s²) - Bumps	Total acceleration a_v (m/s²) - Class C Road
Active Seat	0.0575	0.1736
Active Suspension	0.0465	0.7003
Passive	0.1879	0.8685

The results of Tab.1 are found coherent with other previous studies. (Nagarkar et al., 2018) simulated a vehicle with similar properties to the one on this work through a class C road. They obtained a total acceleration in the vehicle seat of 0.94 m/s² for the passive suspension and 0.65 m/s² for the active suspension with an optimized LQR control. (Alfadhli et al., 2018) also achieved close results, with an RMS of 0.866 m/s² for a passive vehicle and 0.46 m/s² for an active seat. In

this case, the active seat does not attenuate the vibrations so efficiently, but this is due to actuator force limitations imposed by the authors.

In the discussion of ride safety, the deflection of the tires along the simulations must be analyzed. The approach of simulating the tire as a spring requires checking the spring will only have compressing forces, not being able to actuate if the tire loses contact with the ground. This will occur when the tire deflection reaches the static deflection or the value that the tire compresses with only the vehicle weight. Considering the static deflection as the equilibrium position, Table 2 contains important information to evaluate vehicle handling concerning all tires. It's important to highlight that the values are considering the compression as positive values, which means that negative values indicate that the tire has lost contact with the ground. The static deflections are 49.81 mm for the front axle tires and 63.12 mm for the rear axle tires.

Table 2 – Tire Deflection parameters

Case	Bumps			Class C Road		
	RMS	Max. Deflection	Min. Deflection	RMS	Max. Deflection	Min. Deflection
Active Seat	56.90 mm	72.08 mm	40.96 mm	56.99 mm	73.46 mm	33.72 mm
Active Suspension	56.86 mm	65.51 mm	46.38 mm	56.96 mm	73.22 mm	37.72 mm
Passive	56.89 mm	71.72 mm	40.82 mm	57.02 mm	76.2 mm	33.06 mm

From the results of Table 2, it can be seen that the active seat does not have an influent role in tire deflection, which was expected due to the position of the actuator. An active suspension can keep the tire closer to its static position, but in this case, this influence is very small. Again, this can be expected as (Shirahatt et al., 2008) only tuned the LQR controller regarding passenger comfort. In a general picture, the active seat achieved great attenuations in the vibrations transmitted to the seat, as long as it could keep the tires with reasonable deflections to maintain vehicle handling and safety. These statements can confirm the main objective to replace an active suspension with only an active seat to reduce energy consumption and maintain the comfort of the driver.

CONCLUSIONS

In this work, an analysis of active and passive systems to attenuate vehicle vibrations was performed. Concerning the active systems, a solution with four actuators on vehicle suspension and a solution with just one actuator on the vehicle seat were constructed and compared. It was found that both active systems have the potential to attenuate a significant value of the vibrations transmitted to the vehicle seat. Active suspensions performed better at bumps due to their capacity to attenuate the system faster than vehicle seat, consuming 160% more energy. On the other hand, in random excitations, the actuation directly on the seat gives a smoother displacement time-history, translated into a significantly lower acceleration on the seat, consuming 95% less energy than the active suspension. So, we can conclude that active seats are a viable solution for attenuation of vibration on vehicles and can potentially outcome current active systems issues such as financial costs and high energy consumption.

ACKNOWLEDGMENTS

This work was supported by Conselho Nacional de Desenvolvimento Científico e Tecnológico (CNPq/Brazil) grant 140083/2022-7.

REFERENCES

Al-Ashmori, M., and Wang, X. (2020). "A systematic literature review of various control techniques for active seat suspension systems." Applied Sciences (Switzerland), 10(3). https://doi.org/10.3390/app10031148

Alfadhli, A., Darling, J., and Hillis, A. J. (2018). "An active seat controller with vehicle suspension feedforward and feedback states: An experimental study." Applied Sciences (Switzerland), 8(4), 1–22. https://doi.org/10.3390/app8040603

Chen, C. C., and Chen, Y. T. (2021). "Global optimization control for nonlinear full-car active suspension system with multi-performances." In *IET Control Theory and Applications* (Vol. 15, Issue 14, pp. 1882–1905). https://doi.org/10.1049/cth2.12167

Colpo, L. R., and de Souza, C. E. (2020). "Assessment of adjustable damping in the ride comfort of a baja SAE vehicle." Journal of the Brazilian Society of Mechanical Sciences and Engineering, 42(11), 583. https://doi.org/10.1007/s40430-020-02660-4

Ferdek, U., and Łuczko, J. (2018). "Nonlinear modeling and analysis of a shock absorber with a bypass." Journal of

Theoretical and Applied Mechanics (Poland), 56(3), 615–629. https://doi.org/10.15632/jtam-pl.56.3.615

Haemers, M., Derammelaere, S., Ionescu, C.-M., Stockman, K., De Viaene, J., and Verbelen, F. (2018). "Proportional-Integral State-Feedback Controller Optimization for a Full-Car Active Suspension Setup using a Genetic Algorithm." IFAC-PapersOnLine, 51(4), 1–6. https://doi.org/10.1016/j.ifacol.2018.06.004

Hasbullah, F., and Faris, W. F. (2010). "A comparative analysis of LQR and fuzzy logic controller for active suspension using half-car model." 11th International Conference on Control, Automation, Robotics and Vision, ICARCV 2010, *December*, 2415–2420. https://doi.org/10.1109/ICARCV.2010.5707260

Heidarian, A., and Wang, X. (2019). "Review on seat suspension system technology development." Applied Sciences (Switzerland), 9(14). https://doi.org/10.3390/app9142834

Ho, C. M., and Ahn, K. K. (2021). "Design of an Adaptive Fuzzy Observer-Based Fault Tolerant Controller for Pneumatic Active Suspension With Displacement Constraint." IEEE Access, 9, 136346–136359. https://doi.org/10.1109/access.2021.3115909

Jia, H., Yun, C., and Wang, Y. (2019). "Dynamic characteristics analysis of nonlinear suspension system of automobile with seven degrees of freedom." Journal of Physics: Conference Series, 1303(1). https://doi.org/10.1088/1742-6596/1303/1/012049

Karen, I., Kaya, N., Öztürk, F., Korkmaz, I., Yildizhan, M., and Yurttaç, A. (2012). "A design tool to evaluate the vehicle ride comfort characteristics: Modeling, physical testing, and analysis." International Journal of Advanced Manufacturing Technology, 60(5–8), 755–763. https://doi.org/10.1007/s00170-011-3592-z

Kieneke, R., Graf, C., and Maas, J. (2013). "Active seat suspension with two degrees of freedom for military vehicles." IFAC Proceedings Volumes (IFAC-PapersOnline), 46(5), 523–529. https://doi.org/10.3182/20130410-3-CN-2034.00085

Li, W., Dong, X., Yu, J., Xi, J., and Pan, C. (2021). "Vibration control of vehicle suspension with magneto-rheological variable damping and inertia." Journal of Intelligent Material Systems and Structures, 32(13), 1484–1503. https://doi.org/10.1177/1045389X20983885

Liu, H., Gao, H., and Li, P. (2013). "Handbook of vehicle suspension control systems." In *Handbook of Vehicle Suspension Control Systems*. https://doi.org/10.1049/PBCE092E

Łuczko, J., and Ferdek, U. (2020). "Nonlinear dynamics of a vehicle with a displacement-sensitive mono-tube shock absorber." Nonlinear Dynamics. https://doi.org/10.1007/s11071-020-05532-7

Mahala, M. K., Gadkari, P., and Deb, A. (2009). "Mathematical models for designing vehicles for ride comfort." CPDM, Indian Institute of Science, *i*, 168–175.

Nagarkar, M., Bhalerao, Y., Patil, G. V., and Patil, R. Z. (2018). "Multi-Objective Optimization of Nonlinear Quarter Car Suspension System – PID and LQR Control." Procedia Manufacturing, 20, 420–427. https://doi.org/10.1016/j.promfg.2018.02.061

Patelli, G., Morioka, M., and Griffin, M. J. (2018). "Frequency-dependence of discomfort caused by vibration and mechanical shocks." Ergonomics, 61(8), 1102–1115. https://doi.org/10.1080/00140139.2018.1429674

S., G. P., and K., M. M. (2019). "A contemporary adaptive air suspension using LQR control for passenger vehicles." ISA Transactions, 93, 244–254. https://doi.org/10.1016/j.isatra.2019.02.031

Sam, Y. M., Ghani, M. R. H. A., and Ahmad, N. (2000). "LQR controller for active car suspension." IEEE Region 10 Annual International Conference, Proceedings/TENCON, 1. https://doi.org/10.1109/tencon.2000.893707

Shirahatt, A., Prasad, P. S. S., Panzade, P., and Kulkarni, M. M. (2008). "Optimal design of passenger car suspension for ride and road holding." Journal of the Brazilian Society of Mechanical Sciences and Engineering, 30(1), 66–76. https://doi.org/10.1590/s1678-58782008000100010

Xue, X. D., Cheng, K. W. E., Zhang, Z., Lin, J. K., Wang, D. H., Bao, Y. J., Wong, M. K., and Cheung, N. (2011). "Study of art of automotive active suspensions." 2011 4th International Conference on Power Electronics Systems and Applications, PESA 2011. https://doi.org/10.1109/PESA.2011.5982958

Yu, J. H., Lee, K. C., Park, H. B., Choi, Y. G., and Ryu, K. H. (2008). "Development of 2-DOF active seat suspension system for agricultural tractor - design of mechanism and controller." American Society of Agricultural and Biological Engineers Annual International Meeting 2008, ASABE 2008, 5, 3187–3200. https://doi.org/10.13031/2013.25007

RESPONSIBILITY NOTICE

The authors are the only parties responsible for the printed material included in this paper.